

Cortico-striatal functional connectivity predicts transition to chronic back pain

Marwan N Baliki¹, Bogdan Petre¹, Souraya Torbey¹, Kristina M Herrmann¹, Lejian Huang¹, Thomas J Schnitzer², Howard L Fields³ & A Vania Apkarian^{1,4}

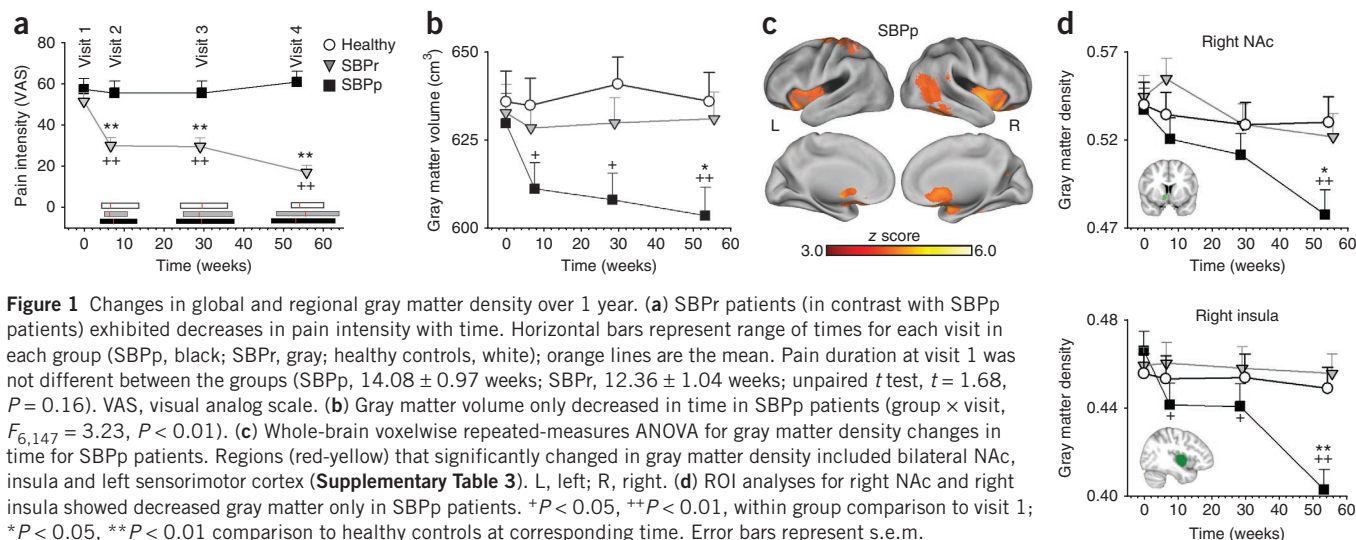
The mechanism of brain reorganization in pain chronification is unknown. In a longitudinal brain imaging study, subacute back pain (SBP) patients were followed over the course of 1 year. When pain persisted (SBPp, in contrast to recovering SBP and healthy controls), brain gray matter density decreased. Initially greater functional connectivity of nucleus accumbens with prefrontal cortex predicted pain persistence, implying that cortico-striatal circuitry is causally involved in the transition from acute to chronic pain.

Although human brain imaging studies have found changes in brain structure and function that correlate with persistent pain¹, the causal relationship between brain reorganization and pain persistence is unknown. Furthermore, changes that precede, and therefore predict, the transition to chronicity have not yet been identified^{2,3}.

We studied subjects following an episode of SBP lasting 4–16 weeks, with no prior back pain for at least 1 year. Brain scans were conducted on each subject at study entry and we followed their pain

and brain markers over four visits for 1 year. SBP patients were subdivided (20% change in pain intensity from baseline to 1 year, visits 1 to 4) into recovering (SBPr, $n = 20$) and persisting (SBPp, $n = 19$) patients (Fig. 1a, Supplementary Fig. 1 and Supplementary Table 1). At baseline, SBPp and SBPr patients showed similar pain and mood characteristics except for the affective dimension of pain, which was substantially higher in SBPp than SBPr patients; at visit 4, SBPr subjects showed decreases in most measured parameters (Supplementary Table 2a), indicating recovery from pain.

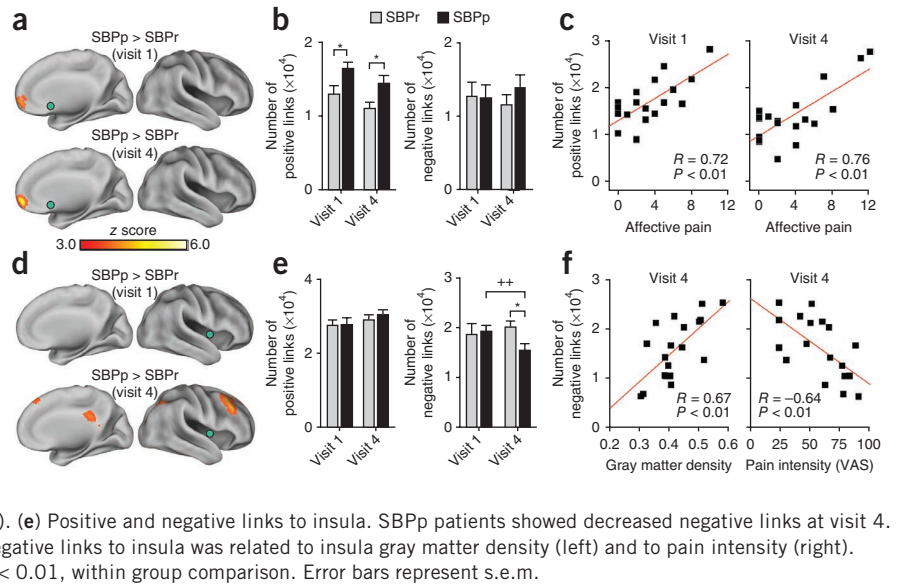
Longitudinal changes in brain structure were assessed using repeated-measure analysis of covariance (ANCOVA), with gender and age as confounds. Consistent with previous findings⁴, SBPp patients exhibited whole-brain gray matter volume decreases over time (Fig. 1b and Supplementary Fig. 2). Healthy controls and SBPp and SBPr patients showed some longitudinal regional gray matter density changes that were similar (Supplementary Figs. 3–5) and were attributable to aging. In addition, SBPp patients showed significant decreases in gray matter density in bilateral striatum (focused in nucleus accumbens (NAC) and extending into caudate and putamen) and insula and in left sensorimotor cortex ($P < 0.01$, corrected for multiple comparisons; Fig. 1c, Supplementary Fig. 3 and Supplementary Table 3). Region of interest (ROI) analyses for right NAC and right insula showed decreased gray matter only in SBPp patients, longitudinally (Fig. 1d and Supplementary Fig. 4) and cross-sectionally with a significant interaction between group and visits ($F_{6,147} = 3.57$, $P < 0.01$). Similar, but less robust, effects were also seen for



¹Department of Physiology, Northwestern University, Feinberg School of Medicine, Chicago, Illinois, USA. ²Department of Rheumatology, Northwestern University, Feinberg School of Medicine, Chicago, Illinois, USA. ³Department of Neurology and the Ernest Gallo Clinic & Research Center, University of California, San Francisco, Emeryville, California, USA. ⁴Departments of Anesthesia and Surgery, Northwestern University, Feinberg School of Medicine, Chicago, Illinois, USA. Correspondence should be addressed to A.V.A. (a-apkarian@northwestern.edu).

Received 6 March; accepted 6 June; published online 1 July 2012; doi:10.1038/nn.3153

Figure 2 Functional connectivity of NAc and insula. (a) Whole-brain voxelwise contrast of NAc (green) functional connectivity (links) between SBPp and SBPr patients. SBPp showed (red-yellow) significantly stronger positive connections between NAc and mPFC at both visits ($P < 0.05$). (b) Average total number of voxels exhibiting positive ($z(r) > 0.25$) and negative ($z(r) < -0.25$) links to NAc. Positive functional connections were larger in SBPp patients at both visits. (Group $F_{1,34} = 8.80$, $P < 0.01$). (c) In SBPp patients, the number of NAc positive links correlated with affective pain (computed from the affective descriptors of McGill pain questionnaire at the day of the scan) at both visits. (d) Whole-brain voxelwise contrast of insula (green) functional connectivity. SBPp showed decreased negative correlations between insula dorsolateral PFC and posterior cingulate cortex in time (group \times visit, $F_{1,34} = 4.04$, $P < 0.05$). (e) Positive and negative links to insula. SBPp patients showed decreased negative links at visit 4. (f) In SBPp patients and at visit 4, the number of negative links to insula was related to insula gray matter density (left) and to pain intensity (right). * $P < 0.05$ in comparison with healthy controls, ** $P < 0.01$, within group comparison. Error bars represent s.e.m.



left sensorimotor cortex (Supplementary Fig. 4). Overall, only SBPp patients exhibited early, localized gray matter loss.

As the NAc is part of the mesolimbic circuitry underlying reinforcement learning (the coordinates of NAc used here when tested in meta-analysis with the word “reward” gives a z score of 15.0 for the association⁵), its functional properties could illuminate the circuitry that mediates learning in pain chronification. In fact, the NAc exhibited significant positive connectivity to bilateral basal ganglia and medial prefrontal cortex (mPFC) in both SBPp and SBPr patients ($P < 0.01$, corrected for multiple comparisons; Supplementary Fig. 5a). The contrast between SBPp and SBPr patients at baseline and at 1 year identified a strengthened mPFC connection to NAc (Fig. 2a and Supplementary Fig. 5b). The NAc exhibited significantly higher positive functional connectivity (with basal ganglia and mPFC) in SBPp patients at baseline and at 1 year ($P < 0.05$; Fig. 2b). Furthermore, the number of positive connections showed a significant relation to affective pain (the only pain parameter that differed between groups at visit 1) at visit 1 that was maintained at visit 4 ($P < 0.01$; Fig. 2c). NAc functional connectivity therefore differs between SBPp and SBPr patients; it is observed at the earliest time point available (when NAc gray matter density did not differ between groups) and persists for 1 year.

At baseline, the insula showed both positive and negative functional connectivity to multiple cortical regions, in both SBPp and

SBPr patients (Supplementary Fig. 6a). At the 1-year follow-up visit, there was decreased negative functional connectivity in SBPp patients between insula and dorsolateral PFC and precuneus (Fig. 2d,e and Supplementary Fig. 6b). This reduced functional connectivity was related positively with insula gray matter density and negatively with pain intensity (Fig. 2f). Functional connectivity of sensorimotor cortex in relation to local gray matter density and pain was similar to that observed for the insula, but with smaller effect sizes (Supplementary Fig. 7). These results imply that the functional reorganization of the insula and sensorimotor cortex are coupled with gray matter changes and directly relate to the persistence of pain.

Our previous findings implicate NAc, mPFC and their functional connectivity (mPFC-NAc) in chronic pain^{6,7}. Here mPFC-NAc functional connectivity was substantially higher in SBPp patients than in SBPr patients at visits 1 and 4 ($P < 0.05$). mPFC-NAc values from a separate scan at baseline (visit 1') predicted future SBP groupings (using receiver operator curves (ROC), and the areas under the curve as discrimination indices, D) best for visit 4 (with $D = 0.83$, $P < 0.01$, unbiased estimate; Fig. 3a–c), with prediction improving at longer times from the initial inciting event. In a separate validation cohort of SBP, we examined baseline mPFC-NAc functional connectivity to predict groupings at 1 year and obtained a similar discrimination (Fig. 3d and Supplementary Fig. 3b). Brain-derived predictability was compared with pain parameters and with a multiple regression model incorporating mPFC-NAc, pain and drug therapy; in all cases, the mPFC-NAc functional connectivity strength was the dominant predictor of pain persistence (Supplementary Table 4a,b).

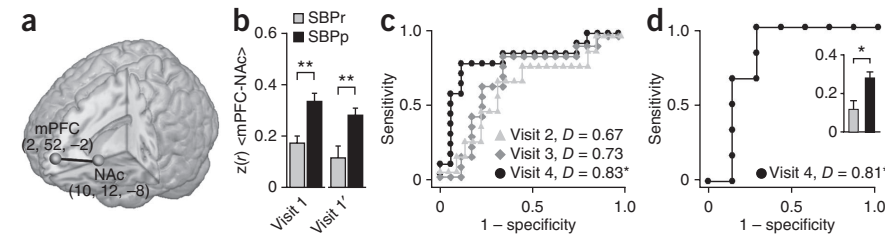


Figure 3 mPFC-NAc functional connectivity predicts pain chronification. (a) Location and coordinates of the mPFC and NAc seeds that we used. (b) mPFC-NAc functional connectivity in SBPp patients was higher than that in SBPr patients in separate fMRI scans. (c) ROC curves and discrimination probabilities (D , area under ROC curve) for predicting pain persistence at visits 2, 3 and 4 using mPFC-NAc at visit 1' (unbiased estimate). (d) In a separate validation group ($n = 13$), mPFC-NAc strengths at visit 1 (inset) and ROC and D values at visit 1 predicted persistence of pain at visit 4. * $P < 0.05$, ** $P < 0.001$. Error bars represent s.e.m.

These results provide, to the best of our knowledge, the first temporal profile of brain parameters during pain chronification. Across all measures and time points, SBPr patients resembled healthy controls, whereas specific changes differentiated SBPp patients. Sensorimotor areas (insula, sensorimotor cortex) and a key mesolimbic (NAc) region showed decreased gray matter density in subjects with persistent pain. Insular cortex function in pain perception is well

documented^{1,8,9}, and insular cortex is activated transiently with pain in patients suffering from chronic back pain⁶. This suggests a direct insular contribution to pain chronification. The role of sensorimotor cortex in pain persistence is less certain. Sensorimotor cortical thickness recovers following effective treatment of CBP¹⁰, and SBPp reorganization for sensorimotor cortex was related to pain; however, postural and tactile modifications secondary to pain persistence may be causal to the observed changes. Decreased negative connectivity of the insula and sensorimotor cortex to other cortical and to thalamic targets may contribute to back pain persistence through diminished cognitive control or by directly enhancing ascending transmission.

The NAc is activated by pain predictive cues and dopaminergic inputs to NAc signal both punishment and reward^{11–13}. Furthermore, mPFC-NAc connectivity and mPFC activity at coordinates that closely match the mPFC-NAc that we studied reflect the intensity of back pain^{6,7}. The mPFC encompassed rostral anterior cingulate, a region involved in human acute and chronic pain conditions¹. In addition, in rodents this region is necessary and sufficient for associating pain with contextual cues¹⁴. These observations, along with our results, indicate that properties and changes in mPFC/anterior cingulate and NAc circuitry are critical for the transition to chronic pain.

Current ideas regarding pain chronification have focused on peripheral nerve and spinal cord reorganization³. We found that the corticolimbic mPFC-NAc connection is an accurate predictor of the transition from subacute to chronic pain. That motivation-valuation circuitry predicts pain persistence raises the possibility that, as with positive reinforcement learning, the NAc contributes to an aversive teaching signal that leads to sustained pain intensity over time following a static peripheral injury.

METHODS

Methods and any associated references are available in the online version of the paper.

Note: Supplementary information is available in the online version of the paper.

ACKNOWLEDGMENTS

We thank all of the patients and healthy volunteers that participated in the study. The study was funded by the National Institute of Neurological Disorders and Stroke (NS35115). M.N.B. was funded by an anonymous foundation.

AUTHOR CONTRIBUTIONS

M.N.B. conducted the experiment, analyzed the data and prepared and wrote the manuscript. B.P. contributed to data collection and analysis. S.T. recruited subjects and conducted the experiment. K.M.H. contributed to data collection. L.H. performed data quality control. T.J.S. recruited subjects and edited the manuscript. H.L.F. wrote the manuscript. A.V.A. designed and supervised the experiment and wrote the manuscript.

COMPETING FINANCIAL INTERESTS

The authors declare no competing financial interests.

Published online at <http://www.nature.com/doi/10.1038/nn.3153>.

Reprints and permissions information is available online at <http://www.nature.com/reprints/index.html>.

1. Apkarian, A.V., Hashmi, J.A. & Baliki, M.N. *Pain* **152**, S49–S64 (2011).
2. Chou, R. & Shekelle, P. *J. Am. Med. Assoc.* **303**, 1295–1302 (2010).
3. Woolf, C.J. & Salter, M.W. *Science* **288**, 1765–1769 (2000).
4. Baliki, M.N., Schnitzer, T.J., Bauer, W.R. & Apkarian, A.V. *PLoS ONE* **6**, e26010 (2011).
5. Yarkoni, T., Poldrack, R.A., Nichols, T.E., Van Essen, D.C. & Wager, T.D. *Nat. Methods* **8**, 665–670 (2011).
6. Baliki, M.N. *et al. J. Neurosci.* **26**, 12165–12173 (2006).
7. Baliki, M.N., Geha, P.Y., Fields, H.L. & Apkarian, A.V. *Neuron* **66**, 149–160 (2010).
8. Baliki, M.N., Geha, P.Y. & Apkarian, A.V. *J. Neurophysiol.* **101**, 875–887 (2009).
9. Isnard, J., Magnin, M., Jung, J., Mauguière, F. & Garcia-Larrea, L. *Pain* **152**, 946–951 (2011).
10. Seminowicz, D.A. *et al. J. Neurosci.* **31**, 7540–7550 (2011).
11. Ungless, M.A., Magill, P.J. & Bolam, J.P. *Science* **303**, 2040–2042 (2004).
12. Seymour, B. *et al. Nature* **429**, 664–667 (2004).
13. Zubieta, J.K. *et al. J. Neurosci.* **25**, 7754–7762 (2005).
14. Johansen, J.P. & Fields, H.L. *Nat. Neurosci.* **7**, 398–403 (2004).

ONLINE METHODS

Subjects. The data presented here are part of an ongoing study in which we examine longitudinal changes in brain structure and function in SBP patients. We initially recruited 120 SBP patients and 31 healthy controls into the study. All participants are right-handed and were diagnosed by a clinician for back pain. An additional list of criteria was imposed, including pain intensity greater than 40/100 on the visual analog scale and duration of less than 16 weeks. Subjects were excluded if they reported other chronic painful conditions, systemic disease, history of head injury, psychiatric diseases or more than mild depression (score >19), as defined by Beck's Depression Inventory. Of the subjects recruited, 17 healthy subjects (7 females, 37.7 ± 1.8 years) and 39 SBP patients (20 females, 40.9 ± 2.3 years) and an additional 13 SBP patients (6 females, 42.3 ± 2.9 years; used for outcome validation) completed this study. Of the subjects recruited, 34 SBP and 7 healthy subjects dropped out or were removed by visit 2, 22 SBP and 1 healthy subject by visit 3, and 10 SBP patients by visit 4. Some SBP patients who completed the study were removed from the analysis because of missing data. The study was approved by the Institutional Review Board of Northwestern University.

All SBP subjects were scanned as soon as possible (mean ± s.e.m. pain duration from injury at visit 1 = 13.15 ± 0.65 weeks) and were followed over the next year (visit 2, 7.15 ± 0.45 weeks; visit 3, 29.20 ± 0.97 weeks; visit 4: 54.36 ± 0.97 weeks; mean ± s.e.m. from visit 1). In addition, healthy controls were scanned four times at similar intervals; for demographics see **Supplementary Table 1**. Dates of visits are shown for all subjects in **Supplementary Figure 1a**.

Pain and mood parameters. For all visits SBP patients completed the short form of the McGill pain questionnaire (MPQ). The main component of the MPQ consists of 12 sensory and 4 affective descriptors, which are used to compute the sensory and affective scores, respectively. Radiculopathy scores were quantified from pain locations that patients had shaded in with pencil on the MPQ form¹⁵. Patients also completed the Positive Affect Negative Affect Score (PANAS), which includes 60 items and measures the two order scales for positive and negative affect. Depression scores were assessed using Beck's Depression Inventory. All questionnaires were given 1 h before brain scanning. Pain and mood parameters for SBPp and SBPr and the differences between the two groups at visits 1 and 4 are presented in **Supplementary Tables 2a and 2b**.

Medication. 34 patients primarily used acetaminophen and NSAIDs (ibuprofen, Motrin, Aleve, Naproxen, Tylenol). Six patients also used opiates (Vicodin or Percocet). One subject used epidural steroid shots (Tramadol), SNRIs (Effexor and pregabalin) and muscle relaxants (cyclobenzaprine). Five patients received no treatment. Patients were subdivided into early (treatment commencement before visit 1) or late (treatment commencement post visit 1) drug groups. Drug consumption at each visit was quantified using the Medication Quantification Scale, which computes a scalar value representation of dosage and duration of drug use.

Scanning parameters. For all participants and visits, MPRAGE type T1-anatomical brain images were acquired with a 3T Siemens Trio whole-body scanner with echo-planar imaging capability using the standard radio-frequency head coil with the following parameters: voxel size = 1 × 1 × 1 mm, repetition time = 2,500 ms, echo time = 3.36 ms, flip angle = 9°, in-plane matrix resolution = 256 × 256; 160 slices, field of view = 256 mm. fMRI images were acquired on the same day and scanner with the following parameters: multi-slice T2*-weighted echo-planar images with repetition time = 2.5 s, echo time = 30 ms, flip angle = 90°, number of volumes = 244, slice thickness = 3 mm, in-plane resolution = 64 × 64. The 36 slices covered the whole brain from the cerebellum to the vertex.

Total gray matter volume estimation. Gray matter volume was determined using SIENAX from the FMRIB Software Library (FSL). A standard FSL peripheral gray matter mask was used to limit gray matter volume estimation to the neocortex. Changes in gray matter volume across groups and visits were determined using a repeated-measure ANCOVA with gender and age as confounds, gray matter volume as the dependent variable, visits for scanning (4 levels, within effects interaction) as the independent variable, gender (two levels) and group

(three levels) as the categorical predictors, and age as the continuous predictor. *Post hoc* comparisons between groups were performed using Tukey's HSEM test.

Voxel based morphometry (VBM). Regional gray matter density was assessed with VBM using FSL 4.1.4. First, a left-right-symmetric study-specific gray matter template was built from 57 gray matter native images (19 images were randomly selected from each group to minimize size of population bias) and their respective mirror images that were all affine-registered to a standard gray matter template. The gray matter images were then linearly normalized onto this template. Finally, images were smoothed with isotropic Gaussian kernel (sigma = 4, full-width at half-maximum = 10 mm).

Longitudinal changes in gray matter density were determined using a voxel-wise repeated-measure ANOVA for each group separately. Changes in gray matter density were assessed using permutation-based inference to allow rigorous comparisons of significance in the framework of the general linear model with $P < 0.01$. Group differences were tested against 5,000 random permutations. Significant clusters were identified using a threshold-free cluster enhancement method, which bypasses the arbitrary threshold necessary in methods that use voxel-based thresholding and is more sensitive and interpretable than cluster-based thresholding methods¹⁶. Differences in gray matter density changes across group and visits were performed using the ROI analysis described below.

fMRI data acquisition and preprocessing. During scanning, patients used a finger-spanning device to continuously rate and log the rate of their spontaneous back pain on a scale of 0–100 in the absence of external stimulation⁶. Two functional scans were collected for each patient at visit 1. These fMRI are labeled visit 1 and visit 1' in **Figure 3**.

The pre-processing of each subject's time series of fMRI volumes was performed using the FMRIB Expert Analysis Tool (FEAT, www.fmrib.ox.ac.uk/fsl) and encompassed skull extraction using the brain extraction tool (BET) from FSL, slice time correction, motion correction, spatial smoothing using a Gaussian kernel of full-width half-maximum of 5 mm and nonlinear high-pass temporal filtering (150 s). The first four volumes were removed to allow for signal stabilization. Several sources of noise were removed through linear regression. These included the six parameters obtained by rigid body correction of head motion, the whole-brain signal averaged over all voxels of the brain, signal from a ventricular ROI and signal from a region centered in the white matter.

Functional connectivity analysis. Functional correlation maps were produced using a well-validated method^{17,18}. Correlation maps were produced by first extracting the BOLD time course from a predetermined functional ROI (fROI) and then computing the correlation coefficient between its time course and the time variability of all other brain voxels. Correlation coefficients were converted to a normal distribution using Fischer's z transform. A two-sided unpaired t test was used to compute significant differences in correlations (Fischer z -transformed values) between the SBPr and SBPp groups using a random effects analysis (z score > 3.0, cluster threshold $P < 0.01$, cluster-based corrected for multiple comparisons).

ROI analysis. Anatomical ROIs (aROI) were defined from the VBM longitudinal analysis and encompassed all statistically significant voxels in an anatomical defined region of the Harvard-Oxford Structural Atlas (**Supplementary Fig. 4**). The gray matter density for a given aROI was determined by averaging the gray matter density for all voxels in the given ROI. Differences in gray matter density across groups and visits were determined using a repeated-measure ANCOVA with gender and age as confounds (same design as used for whole-brain gray matter volume).

fROIs were also determined from the VBM longitudinal analysis and were defined as 10-mm spheres centered on the voxel showing greatest longitudinal gray matter density change for each of the right NAc ($x = 10, y = 12, z = -8$), right insula ($x = 40, y = -6, z = -2$) and left sensorimotor cortex ($x = -32, y = -34, z = 66$). An additional fROI in the mPFC ($x = 2, y = 52, z = -2$) was defined from the right NAc functional connectivity contrast map (SBPp > SBPr). The number of positives and negatives links for a given ROI were computed by transforming functional connectivity maps of an ROI into standard MNI space and counting the number of voxels in the whole brain with $z(r) > 0.25$ (positive links) or $z(r) < -0.25$ (negative links). Differences in number of positive and negative links across groups and visits were determined using a repeated-measure ANCOVA

with gender and age as confounds (same design as for whole-brain gray matter volume). The contribution of head motion (**Supplementary Fig. 8**) and medication use (**Supplementary Fig. 9**) were studied as confounds, and showed minimal influence on reported results.

15. Chanda, M.L. *et al. J. Pain* **12**, 792–800 (2011).
16. Smith, S.M. & Nichols, T.E. *Neuroimage* **44**, 83–98 (2009).
17. Baliki, M.N., Geha, P.Y., Apkarian, A.V. & Chialvo, D.R. *J. Neurosci.* **28**, 1398–1403 (2008).
18. Fox, M.D. *et al. Proc. Natl. Acad. Sci. USA* **102**, 9673–9678 (2005).